Hysteresis in Ising model in transverse field

1994 J. Phys. A: Math. Gen. 27 1533

(http://iopscience.iop.org/0305-4470/27/5/018)

J. Phys. A: Math. Gen. 27 (1994) 1533–1540. Printed in the UK

Hysteresis in Ising model in transverse field

M Acharyya†, B K Chakrabarti†‡ and R B Stinchcombe‡
† Saha Institute of Nuclear Physics, 1/AF Bidhan Nagar, Calcutta 700064, India
‡ Department of Theoretical Physics, 1 Keble Road, Oxford, OX1 3NP, UK

Received 30 September 1993

Abstract. The hysteretic response of an Ising system to a periodically varying transverse (tunnelling) field has been investigated. Numerical and approximate analytical techniques have been used to solve the mean-field equation for the dynamics, in the presence of a heat bath at a finite temperature. The scaling behaviour of the hysteresis loop area and the phase diagram for the dynamic (phase) transition have been obtained.

1. Introduction

When the external magnetic field on a ferromagnet is swept, say sinusoidally, in time the system cannot respond instantaneously, and the response gets delayed (in general periodically but modified in form for its time variation). In particular, if the relaxation time of the thermodynamic system is larger than the time period of the oscillating magnetic field, an interesting competition takes place. This leads [1] to the hysteresis loops, arising out of the delay in response to the driving field; a typical non-equlibrium phenomena.

There has been considerable investigation in recent years, on the hysteretic response of various (classical) magnetic model systems. Rao *et al* [2] observed the power-law variation of the hysteresis loop area (A) with the (small) frequency (f) and amplitude (h_0) of the externally applied magnetic field, in a n-vector model in the $n \to \infty$ limit. Dhar and Thomas [3] considered the transverse magnetization possible in the n-vector model, and obtained the (corrected) power law in the $n \to \infty$ limit. Tome and de Oliviera [4] studied the (delayed) response of an Ising magnet in the presence of a sinusoidally varying magnetic field, solving numerically the approximate mean-field equation for the Ising dynamics. Lo and Pelcovits [5] studied the Monte Carlo dynamics of an Ising model (in two dimensions) in presence of a sinusoidally varying external field and obtained the power law variation of the loop area A in the f and $h_0 \to 0$ limit. Acharyya and Chakrabarti [1] studied Monte Carlo dynamics of Ising models in one to four dimensions, and also the mean-field equation of motion, for a wide range of variation of frequency and amplitude of external magnetic field and the temperature of the system. They fitted the observed variation of the loop area to a scaling form, with the (non-monotonically varying; Lorentzian in the mean-field limit) scaling function reducing to the previously observed power law in the low frequency limit.

Here we study similar (finite temperature) relaxation and the consequent hysteresis phenomena, in an Ising system put in a periodically varying *transverse* or tunnelling field. Specifically, our system is described by the Hamiltonian

$$H = -\sum_{(i,j)} J_{ij}\sigma^z{}_i\sigma^z{}_j - \Gamma(t)\sum_i \sigma^x{}_i \qquad \Gamma(t) = \Gamma_0 \cos(2\pi f t) \tag{1}$$

where the σ's are the Pauli matrices.

0305-4470/94/051533+08$19.50

In view of the wide applicability of the (time-independent) transverse Ising Hamiltonian to represent the (tunnelling induced) order-disorder transition in hydrogen-bonded (KDP-type) ferroelectrics and Jahn–Teller compounds [6], and the possibility of tuning the transverse (tunnelling) field by changing the external pressure on the hydrogen-bonded ferroelectrics [7], the study of quantum hysteresis in such a transverse Ising model is not just of pedagogic interest. With suitable tuning of the transverse field by pressure modulation, the interesting features of the hysteresis loops in such ferroelectric systems, as obtained here for the above model, can be studied.

We have studied here the variation of the longitudinal and transverse magnetization loop areas $A_x = \oint m^x \mathrm{d}\Gamma$ and $A_z = \oint m^z \mathrm{d}\Gamma$ respectively, and the dynamic order parameter $Q = \oint m^z \mathrm{d}t$, as functions of the frequency (f) and amplitude (Γ_0) of the periodically-varying transverse field and the temperature (T) of the system, from the equation of motion for the average magnetization $m = \langle \sigma_i \rangle = m^x \hat{x} + m^z \hat{z}$. This we have done here by setting up the mean-field equations of motion for the magnetization m.

We find that the variation of the loop area A_x with frequency f, for different parameters (Γ_0 and T) can be expressed in a scaling form. Also, a dynamic phase transition (from $Q = 0$ for high Γ_0 and T) to $Q \neq 0$ (beyond critical values of Γ_0 and T, depending on f) occurs and the phase diagram (in the Γ_0, T plane) for this transition has been obtained.

2. Mean-field equation of motion

In the mean-field approximation [8] (see also [6]), the Hamiltonian can be approximated as

$$H \simeq -\sum_i h_i \cdot \sigma_i \qquad h_i = m_i^z \hat{z} + \Gamma \hat{x} \tag{2}$$

where the nearest neighbour sum over $J_{i,j}$ in (1) has been taken as unity. We then write the generalized mean-field equation of motion (cf [9]) as

$$\tau \frac{\mathrm{d}m}{\mathrm{d}t} = -m + \left[\tanh\left(\frac{|h|}{T}\right)\right] \frac{h}{|h|} \qquad |h| = \sqrt{[(m^z)^2 + \Gamma^2]} \tag{3}$$

where $\Gamma \equiv \Gamma(t)$ is a sinusoidally varying function as given in (1).

It may be mentioned here that the macroscopic relaxation time τ can, in principle, differ for longitudinal and transverse magnetization. In order to reduce the number of free parameters in the Hamiltonian, we have considered them identical here. In the classical limit ($\Gamma = 0$), the above equation of motion reduces to the well known mean-field equation [9] for the Ising dynamics.

3. Numerical results

We solved numerically, using a fourth-order Runge–Kutta method (in single precision; the value of the time differential was taken to be 10^{-5}), the above (coupled) dynamical equations (for the two components of magnetization in (3)). Using a simple trapezoidal rule we then evaluted the longitudinal and transverse magnetic hysteresis-loop area A_x and A_z and the dynamic order parameter Q as defined earlier.

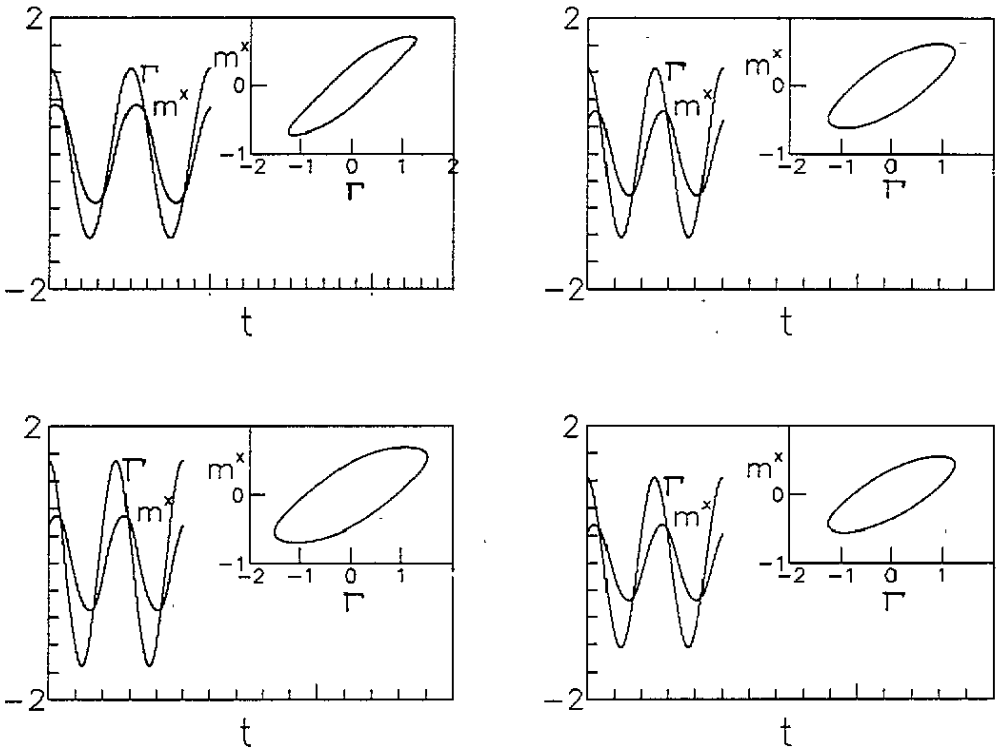

Figure 1. The time variation of the perturbing transverse field (Γ) and the corresponding response for the x-component of magnetization (m^x). The insets shows the corresponding Lissajous plots. (i) $f = 1000$, $\Gamma_0 = 1.25$ and $T = 1.25$; (ii) $f = 2000$, $\Gamma_0 = 1.25$ and $T = 1.25$; (iii) $f = 2000$, $\Gamma_0 = 1.50$ and $T = 1.25$ and (iv) $f = 2000$, $\Gamma_0 = 1.25$ and $T = 1.50$.

Some typical hysteresis loops (for two defferent sets of parameters f, Γ_0 and T) are shown in figure 1 for the x-components of magnetization (m^x) and in figure 2 for the z-component of magnetization (m^z), respectively.

The variation of the loop area A_x with frequency f has been shown in the inset of figure 3, for different amplitude Γ_0 and temperature T. We fitted this variation in the loop area A_x (for comparatively large Γ_0 and T values; in the range 1 to 2 for both the parameters, in figure 3), to the scaling form (1)

$$A_x \sim \Gamma_0^{\alpha} T^{-\beta} g\left(\frac{f}{\Gamma_0^{\gamma} T^{\delta}}\right) \tag{4}$$

with a Lorentzian scaling function

$$g(x) \sim \frac{x}{1 + (cx)^2}. \tag{5}$$

The best-fit values for the exponents α, β, γ and δ are found to be around 1.75 ± 0.05, 0.50 ± 0.02, 0 ± 0.02 and 0 ± 0.02; the data collapse (see figure 3) is very convincing using (4) with these exponent values, but gets visibly disturbed for exponent values beyond the above ranges.

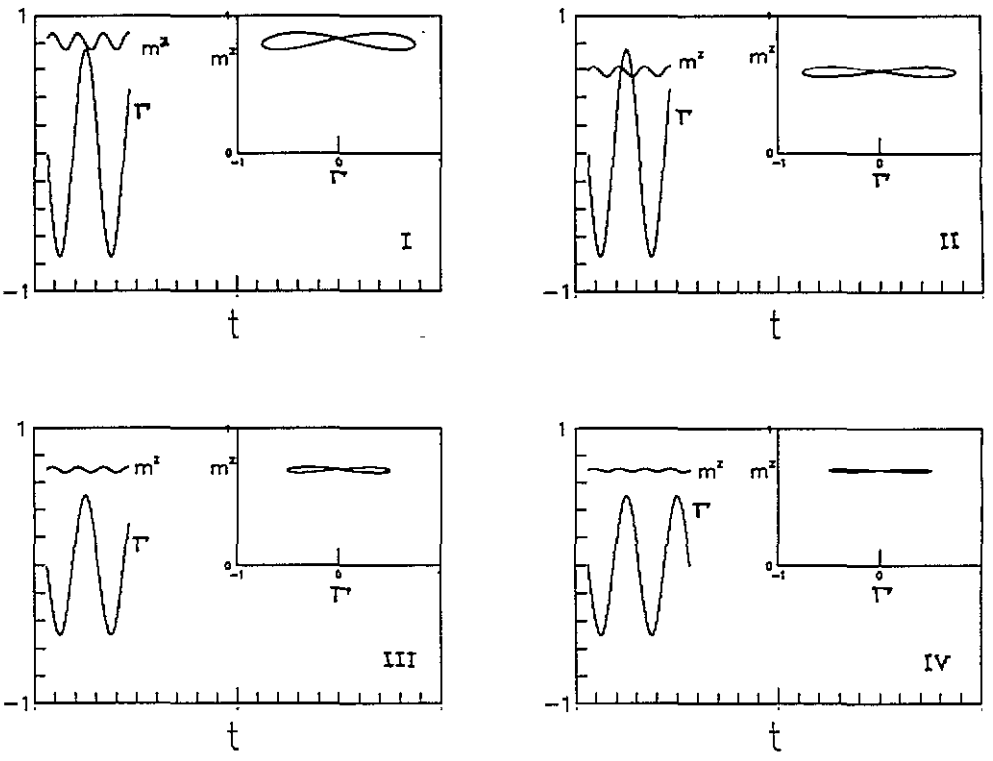

Figure 2. The time variation of the perturbing transverse field (Γ) and the corresponding response for the z-component of magnetization (m^z). The insets show the corresponding Lissajous plots. (i) f = 2000, Γ_0 = 0.75 and T = 0.50; (ii) f = 2000, Γ_0 = 0.75 and T = 0.75; (iii) f = 2000, Γ_0 = 0.50 and T = 0.75 and (iv) f = 4000, Γ_0 = 0.50 and T = 0.75.

It may be mentioned that the loop area A_z does not show up any comparable smooth scaling with frequency, for different parameter values. It may also be noted in this connection that, unlike A_x, A_z loops do not correspond to any energy change.

We also studied the variation of the quantity Q with Γ_0, T and f. We found, that Q decreases continuously with increasing Γ_0 and T. A (dynamic) phase transition from $Q \neq 0$ (for low values of Γ_0 and T) to $Q = 0$ (beyond a phase boundary line) was detected numerically ($Q < 10^{-8}$ for $Q = 0$ phase). This phase separation line is shown in figure 4 for a typical value of f (= 500).

4. Approximate analytic results

Some understanding of this scaling can, in fact, be obtained from line arised forms of the equation of motion (3). Linearization can be carried out in three limits: namely, in the high temperature ($T^{-1} \to 0$), the low tunnelling field amplitude ($\Gamma_0 \to 0$) and in the adiabatic ($f \to 0$) limits.

In the first two cases, the linearized equations of motion take the forms

$$\tau \frac{dm^x}{dt} = -m^x + \frac{\Gamma(t)}{T} \qquad \tau \frac{dm^z}{dt} = -\left(1 - \frac{1}{T}\right) m^z \tag{6}$$

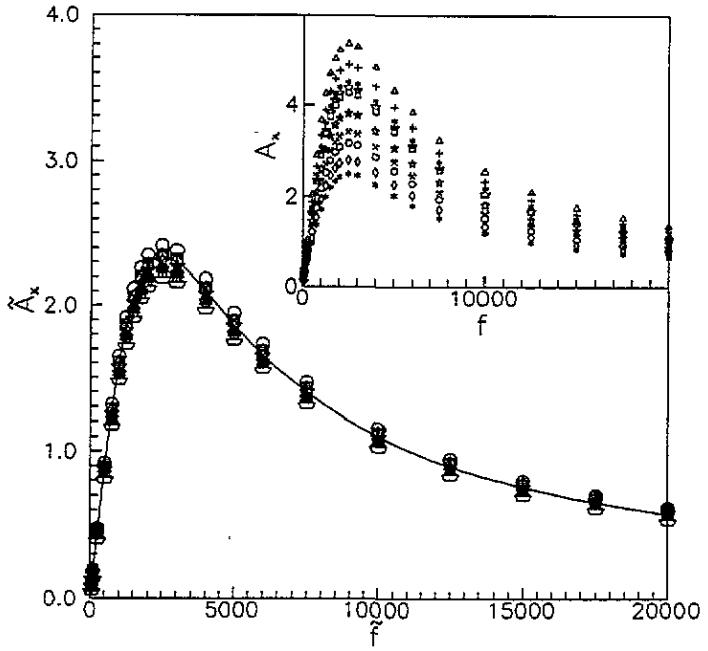

Figure 3. The variation of the scaled loop area $A_x = A_x\Gamma_0^{-\alpha}T^{\beta}$ with the scaled frequency $f = f/(\Gamma_0^{\gamma}T^{\delta})$ using $\alpha = \frac{7}{4}$, $\beta = \frac{1}{2}$ and $\gamma = 0 = \delta$. Different symbols correspond to different Γ_0 and T : (○) $\Gamma_0 = 1.25$ and $T = 1.25$; (□) $\Gamma_0 = 1.50$ and $T = 1.25$; (△) $\Gamma_0 = 1.75$ and $T = 1.25$; (◇) $\Gamma_0 = 1.25$ and $T = 1.50$; (☆) $\Gamma_0 = 1.50$ and $T = 1.50$; (+) $\Gamma_0 = 1.75$ and $T = 1.50$; (*) $\Gamma_0 = 1.25$ and $T = 1.75$; (×) $\Gamma_0 = 1.50$ and $T = 1.75$; (⊞) $\Gamma_0 = 1.75$ and $T = 1.75$. The full curve indicates the proposed Lorentzian scaling function (5). The inset shows the variation of A_x with f at different Γ_0 and T.

in the $T^{-1} \to 0$ limit, and

$$\tau\frac{dm^x}{dt} = -m^x + \left[\tanh\left(\frac{m^z}{T}\right)\right]\frac{\Gamma(t)}{m^z} \qquad \tau\frac{dm^z}{dt} = -m^z + \tanh\left(\frac{m^z}{T}\right) \tag{7}$$

in the $\Gamma_0 \to 0$ limit. For $T > 1$, m^z decays to zero in the first case (6). The long-time solution of the dynamical equation for m^z in [7] can be obtained easily as the attractive fixed point of the map describing the discretized form of the differential equation: $m^z(t+\tau) = \tanh[m^z(t)/T]$. This gives $m^z = \tanh(m^z/T) \neq 0$ for $T < 1$ and $m^z = 0$ for $T > 1$. Putting the solution for m^z for $T < 1$ into the dynamical equation for m^x in (7), reduces it to the same form as (6) but with $\Gamma(t)/T$ now replaced by $\Gamma(t)$ in the second term. Defining now $s \equiv 2\pi ft$ and $\lambda \equiv 2\pi f\tau$, one can express the general solution of $m^x(t)$ as

$$m^x(t) = J\cos(s) + K\sin(s) \tag{8}$$

with $K = \lambda J = (\Gamma_0/T)[\lambda/(1+\lambda^2)]$ for $T > 1$ from (6) as well as from (7), and Γ_0/T replaced by Γ_0 for $T < 1$ (from (7)). The loop area $A_x = \oint m^x d\Gamma = 2K\Gamma_0$ can then be expressed in the form given in (4) (containing the full Lorentzian scaling function $g(\lambda)$). The resulting exponents are $\alpha = 2$, $\beta = 1$ and $\gamma = 0 = \delta$ in the $T^{-1} \to 0$ limit (from (6) and (7) for $T > 1$) and $\alpha = 2$, $\beta = 0 = \gamma = \delta$ in the $\Gamma_0 \to 0$ limit (from (7) for $T < 1$).

In the adiabatic ($f^{-1} \gg \tau$, or small λ) limit, one can write $m = m_0 + \delta + O(\lambda^2)$, where $m_0 \sim O(\lambda^0)$ and $\delta \sim O(\lambda^1)$: $m_0 \equiv [\tanh(|h|/T)](h/|h|)$. Now collecting the linear

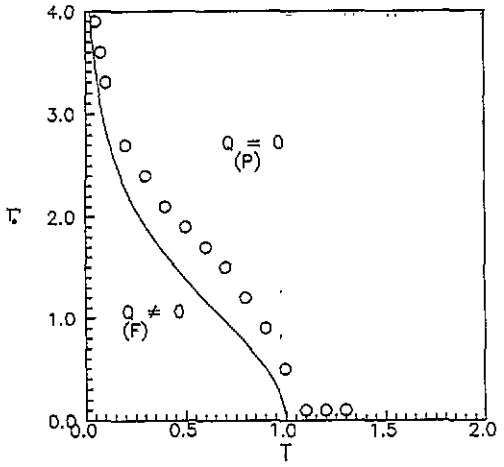

Figure 4. Phase diagram for the dynamic phase transition: below the critical $\Gamma_0^c(T)$ line indicated by the symbols, Q acquires a non-zero value in the 'F' phase and $Q = 0$ in the 'P' phase. The open circles correspond to $Q = 0$ for $f = 500$. The estimate of the phase boundary from (12) has been indicated by the full curve.

terms in δ and λ, one gets

$$\delta^x = -\lambda \frac{\mathrm{d}m_0^x}{\mathrm{d}s} \qquad \delta^z = \frac{\delta^z}{\Gamma} \tanh\left(\frac{\Gamma}{T}\right). \tag{9}$$

For $T > 1$, the above equation gives the solution $\delta^z = 0$ (of course $m_0^z = 0$). Using this to obtain m_0^x for the right-hand side of the other equation, one gets $\delta^x = -\lambda(\mathrm{d}/\mathrm{d}s)\tanh[\Gamma(s)/T]$. Hence the loop area $A_x = \oint m^x \mathrm{d}\Gamma = \oint (m_0^x + \delta^x)\mathrm{d}\Gamma + \mathrm{O}(\lambda^2)$, where $\Gamma = \Gamma_0 \cos(s)$, can be expressed as

$$A_x \sim f \frac{\Gamma_0^2}{T} I\left(\frac{\Gamma_0}{T}\right) + \mathrm{O}(f^2) \qquad \text{where} \quad I(y) = \int_0^{2\pi} \sin^2(s)\,\mathrm{sech}^2[y\cos(s)]\mathrm{d}s\,. \tag{10}$$

As $I(y)$ goes to π and $4/y$ in the small and large y limits, respectively, the loop area A_x can again be expressed in the form (4) with $g(x) \sim x$ in the $x \to 0$ limit, and with $\alpha = 2$, $\beta = 1$, $\gamma = 0 = \delta$ in the $\Gamma_0 \ll T$ limit and with $\alpha = 1$, $\beta = 0 = \gamma = \delta$ in the $\Gamma_0 \gg T$ limit. Although these limiting values for the exponents are not observed (because of the inaccuracy of the linearization approximations in the range of our study), they provide useful bounds for the observed values, and the Lorentzian scaling function appears quite naturally here (without any frequency rescaling ($\gamma = 0 = \delta$), unlike the classical case [1]).

In the $Q \neq 0$ phase in the dynamic phase diagram (figure 4), m^z itself acquires a non-zero amplitude (which vanishes beyond the phase boundary). An equation for the phase boundary can therefore be obtained from the dynamical equation for m^z in (3) by determining the line, approached from large Γ_0 and T region ($m^z = 0$), where m^z tends to grow. Near this line, the dynamical equation for m^z can be integrated over one cycle to obtain

$$\frac{\lambda}{2\pi} \oint \frac{\mathrm{d}m^z}{m^z} = \frac{1}{2\pi} \int_0^{2\pi} \left[\frac{1}{\Gamma(s)} \tanh\left(\frac{\Gamma(s)}{T}\right) - 1\right] \mathrm{d}s \equiv \frac{1}{\Gamma_0} F\left(\frac{\Gamma_0}{T}\right) - 1\,. \tag{11}$$

The right-hand side of (11) is the logarithm of the factor by which m^z grows over one cycle. So, the equation for the phase boundary line (for any finite f) is given by $\Gamma_0 =$

$F(\Gamma_0/T)$. For small y, $F(y) \sim y$, giving the transition at $T = 1$, as $\Gamma_0 \to 0$ (see figure 4). In fact this is an exact point for the phase boundary in the $\Gamma_0 \to 0$ limit, as can be seen from the possibility of linearization of the tanh function in the equation of motion (3) for m^z in this limit when one approaches from the $Q = 0$ ($m^z = 0$) phase. For large y, $| y\cos(s) | \sim y | s - \pi/2 |$, and expanding $\tanh(x)$ as $x/(1 + x^2)^{1/2}$, one gets $F(y) \sim (2/\pi) \sinh^{-1}[(\pi/2)(\Gamma_0/T)]$. This approximation is actually good for all y, and gives the phase boundary equation as

$$T = \frac{(\pi/2)\Gamma_0}{\sinh((\pi/2)\Gamma_0)}. \tag{12}$$

The analytic estimate (from the above equation) for the phase boundary line is shown by the continuous line in figure 4, and gives fair agreement with the numerical results. A similar study here for the transverse magnetization gives $\oint m^x \mathrm{d}t \sim 0$ for the entire parameter space, as the time variation of the transverse magnetization has the antisymmetry of $\Gamma(t)$ (as in figure 1).

5. Concluding remarks

A few concluding remarks are appropriate here. Our study uses the mean-field equation of motion (3). It should be emphasized that other possible forms of the equation of motion can be derived from the mean-field free energy [6]); these however reduce to our form in the high temperature limit, and are expected to give the same qualititative behaviour for the hysteresis. It may also be mentioned that our equation of motion arises solely from 'heat bath' and does not contain any 'intrinsic' dynamics (arising from $[H, \sigma]$). Such quantum dynamics will typically be much more rapid than that considered here, but should be included for other (high frequency and low temperature) regimes.

In conclusion, here we have studied the hysteretic response of the Ising model at a finite temperature, in the presence of a periodically driven transverse field. Solving numerically for the time variation for the response magnetization (from the above equation of motion), we find the transverse magnetization loop area A_x shows a scaling ((4), see figure 3) to a Lorentzian form in the high temperature limit. Also, we observe a dynamic phase transition for the longitudinal magnetization, and the phase boundary obtained here is different from the static one (see figure 4). Approximate analytic techniques have also been used to explore the solution of the dynamical equation (3) in various limits. The analytic results for the loop area A_x in these limits have been compared with the numerically observed scaling behaviour (expressed by (4)). An approximate analytic estimate of the (dynamic) phase boundary has also been obtained (equation (12)) and the results have been compared with the numerical observations.

Acknowledgment

BKC is grateful to the Indian National Science Academy, Delhi, and the Royal Society, London, for financial support.

References

[1] Acharyya M and Chakrabarti B K 1993 *Physica* **192A** 471; 1994 *Physica* **202A** 467
[2] Rao M, Krishnamurthy H R and Pandit R 1989 *J. Phys.: Condens. Matter* **1** 9061; 1990 *Phys. Rev.* B **42** 856
[3] Dhar D and Thomas P B 1992 *J. Phys. A: Math. Gen.* **25** 4967
[4] Tome T and de Oliviera M J 1990 *Phys. Rev.* A **41** 4251
[5] Lo W S and Pelcovits R A 1990 *Phys. Rev.* A **42** 7471
[6] Stinchcombe R B 1973 *J. Phys. C: Solid State Phys.* **6** 2459
[7] Peercy P S 1975 *Phys. Rev.* B **12** 2725
[8] de Gennes P G 1963 *Solid State Commun.* **1** 132
[9] Suzuki M and Kubo R 1968 *J. Phys. Soc. Japan* **24** 51